Espessura elástica efetiva

Espessura elástica efetiva flexura da litosfera

- Upon rifting away from the MOR the lithosphere thickens (the base of the thermal lithosphere is defined by an isotherm, usually $T_m \approx 1300°C$) and subsides, and that the cooled lithosphere is more dense than the underlying mantle. In other words, it forms a gravitationally unstable layer.
- Why does it stay atop the asthenosphere instead of sinking down to produce a more stable density stratification?
- That is because upon cooling the lithosphere also acquires strength. Its weight is supported by its strength; the lithosphere can sustain large stresses before it breaks.
- The initiation of subduction is therefore less trivial than one might think and our understanding of this process is still far from complete.
- **The strength of the lithosphere has important implications:**
- it means that the lithosphere can support loads, for instance by seamounts
- the lithosphere, at least the top half of it, is seismogenic
- lithosphere does not simply sink into the mantle at trenches, but it bends or flexes, so that it influences the style of deformation along convergent plate boundaries.

Espessura elástica efetiva flexura da litosfera

- Investigation of the bending or flexure of the plate provides important information about the mechanical properties of the lithospheric plate. The nature of the bending is largely dependent on the flexural rigidity, D, which in turn depends on the elastic parameters of the lithosphere and on the elastic thickness (Te) of the plate.
- The rheological response of a material to stress depends on the duration of the stress. The reaction to a short-lasting stress, as experienced during the passage of a seismic wave, may be quite different from the reaction of the same material to a steady load applied for a long period of time. This is evident in the different thicknesses obtained for the lithosphere in seismic experiments and in elastic plate modelling.

Espessura elástica efetiva flexura da litosfera

- Para saber de onde vem D e Te

To derive the equations for the bending of a thin elastic plate we need to

1. apply laws for equilibrium: sum of the forces is zero and the sum of all moments is zero: $\sum F = 0$ and $\sum M = 0$
2. define the constitutive relations between applied stress σ and resultant strain ϵ
3. assume that the deflection $w \ll L$, the typical length scale of the system, and h, the thickness of the elastic plate $\ll L$. The latter criterion (#3) is to justify the use of **linear elasticity**.

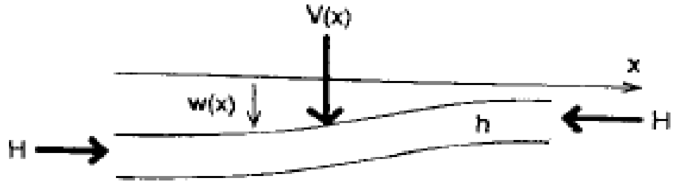

Figure 5.14: Deflection of a plate under a load.

Espessura elástica efetiva flexura da litosfera

In a 2D situation, i.e., there is no change in the direction of y, the bending of a homogeneous, elastic plate due to a load $V(x)$ can be described by the fourth-order differential equation that is well known in elastic beam theory in engineering:

$$D\frac{d^4w}{dx^4} + P\frac{d^2w}{dx^2} = V(x) \qquad (5.28)$$

with $w = w(x)$ the deflection, i.e., the vertical displacement of the plate, which is, in fact, the ocean depth(!), D the **flexural rigidity**, and P a horizontal force.

The flexural rigidity depends on elastic parameters of the plate as well as on the thickness of the plate:

$$D = \frac{Eh^3}{12(1-\nu^2)} \qquad (5.29)$$

with E the Young's modulus and ν the Poisson's ratio, which depend on the elastic moduli μ and λ (See Fowler, Appendix 2).

Espessura elástica efetiva

Global strength and elastic thickness of the lithosphe

Magdala Tesauro [a,b,*], Mikhail K. Kaban [a,c], Sierd A.P.L. Cloetingh [b]

[a] German Research Center for Geosciences (GFZ), Potsdam, Germany
[b] Department of Earth Science, Utrecht University
[c] IPE, Moscow, Russia

Global and Planetary Change 90–91 (2012) 51–57

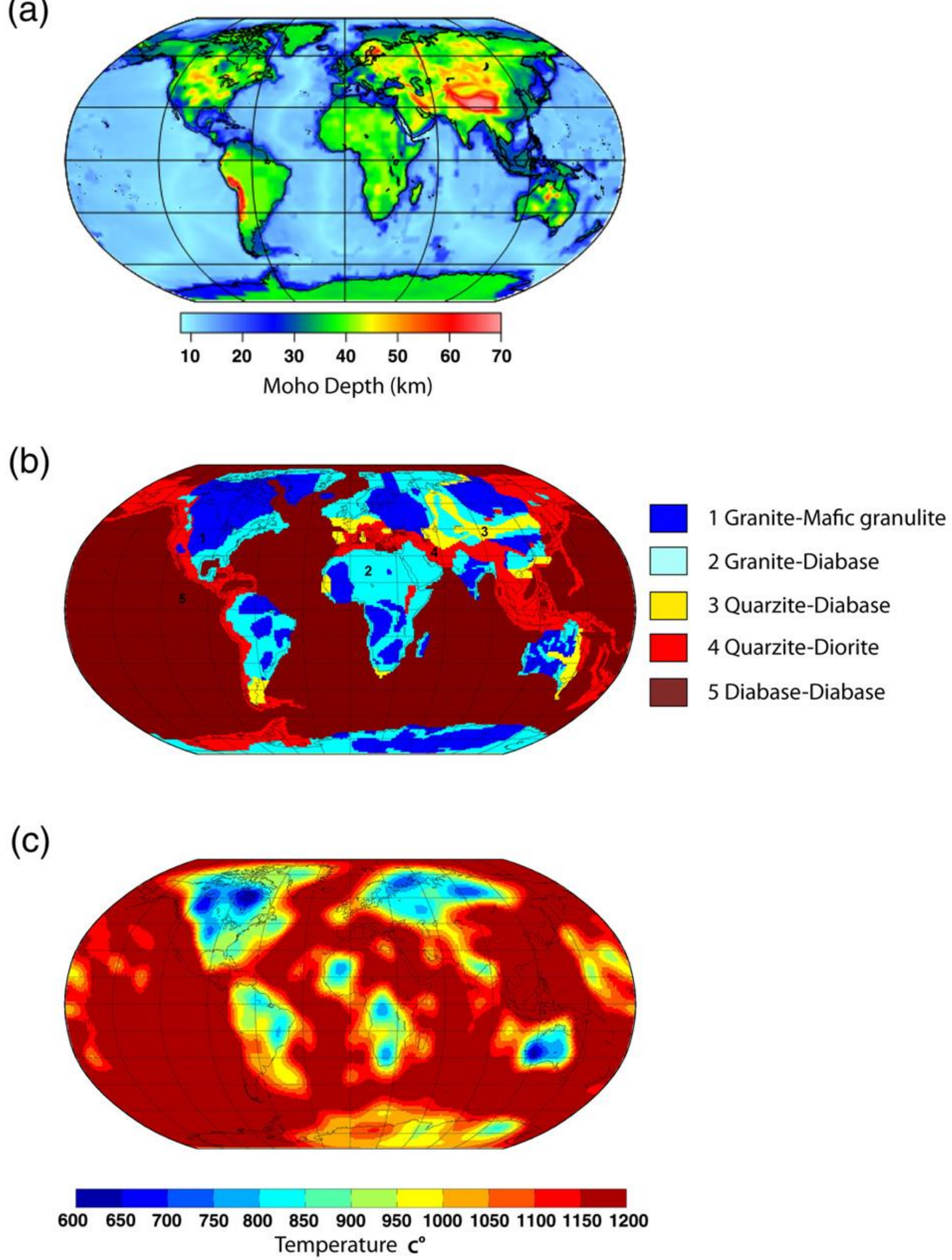

Parâmetros de entrada: (a)Profundidade da Moho (km) – baseado no modelo CRUST2

(b) Tipos reológicos da crosta superior e inferior

We assume different rheologies of the upper and lower continental crust (Fig. 1b) according to the age of the geological provinces (Mooney et al., 2009). In doing so, we associate a 'hard' rheology represented by granite-mafic granulite, to the Achaean and old Proterozoic structures, a 'soft' rheology, represented by quartzite-diorite to the Meso-Cenozoic and an 'average' rheology represented by granite-diabase and quartzite-diabase to the structures of the intermediate age.

(b) Temperatura a 100 km de profundidade a partir de inversão de tomografia.

Fig. 1. (a c) Examples of the main input parameters for the strength estimates. (a) Moho depth (km); (b) Rheological types of the upper and lower crust; (c) Temperature at 100 km depth from inversion of tomographic data (Ritsema et al., 2004).

Fig. 3. (a–c) Integrated strength (Pa m) in compression for (a) the lithosphere and (b) crust; (c) Fraction of the integrated total strength contributed by the crust.

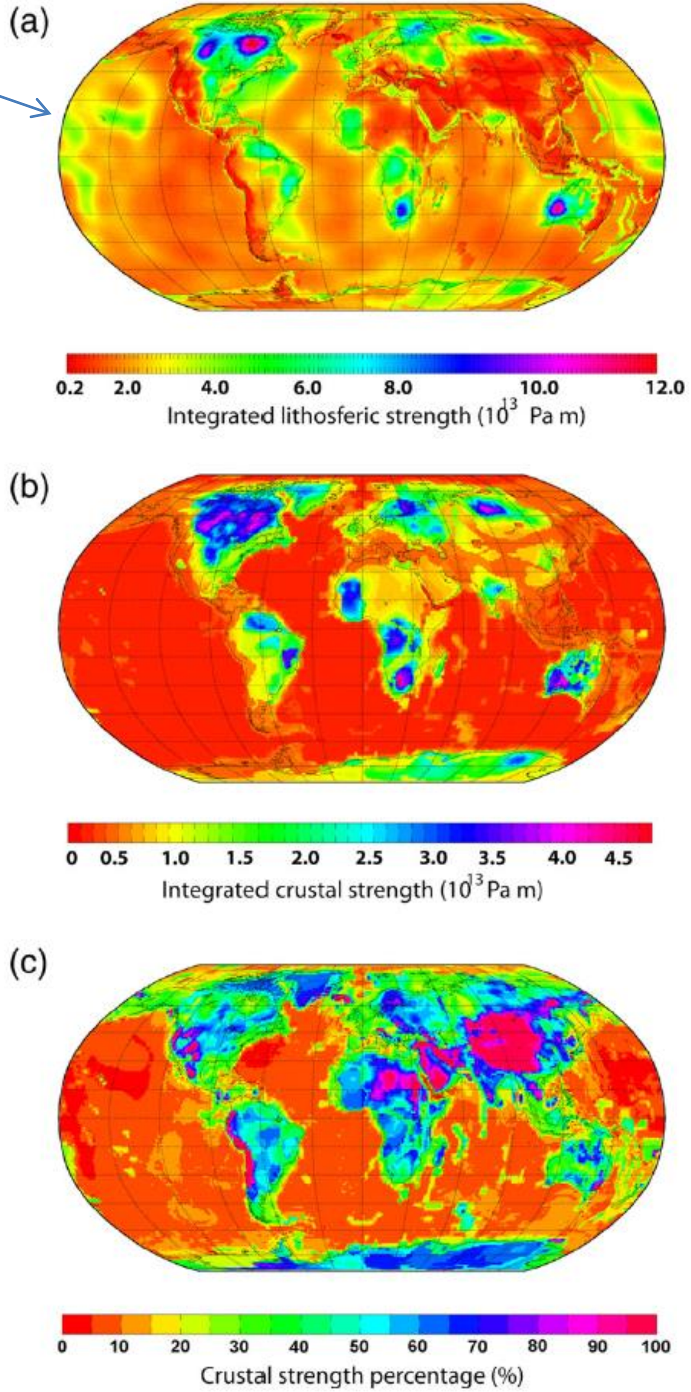

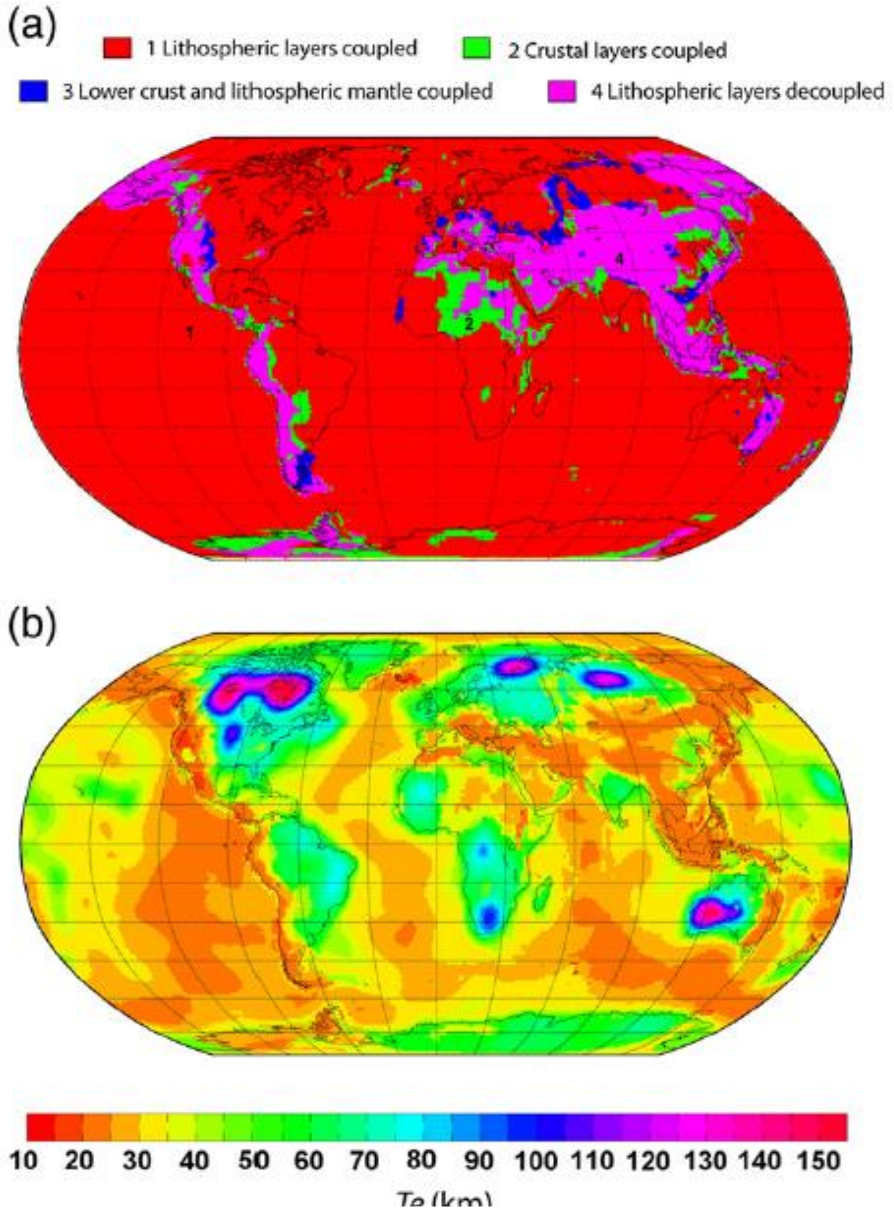

Fig. 4. (a–b) (a) Coupling and decoupling conditions of the lithospheric layers; (b) Effective elastic thickness (*Te*) of the lithosphere (km).

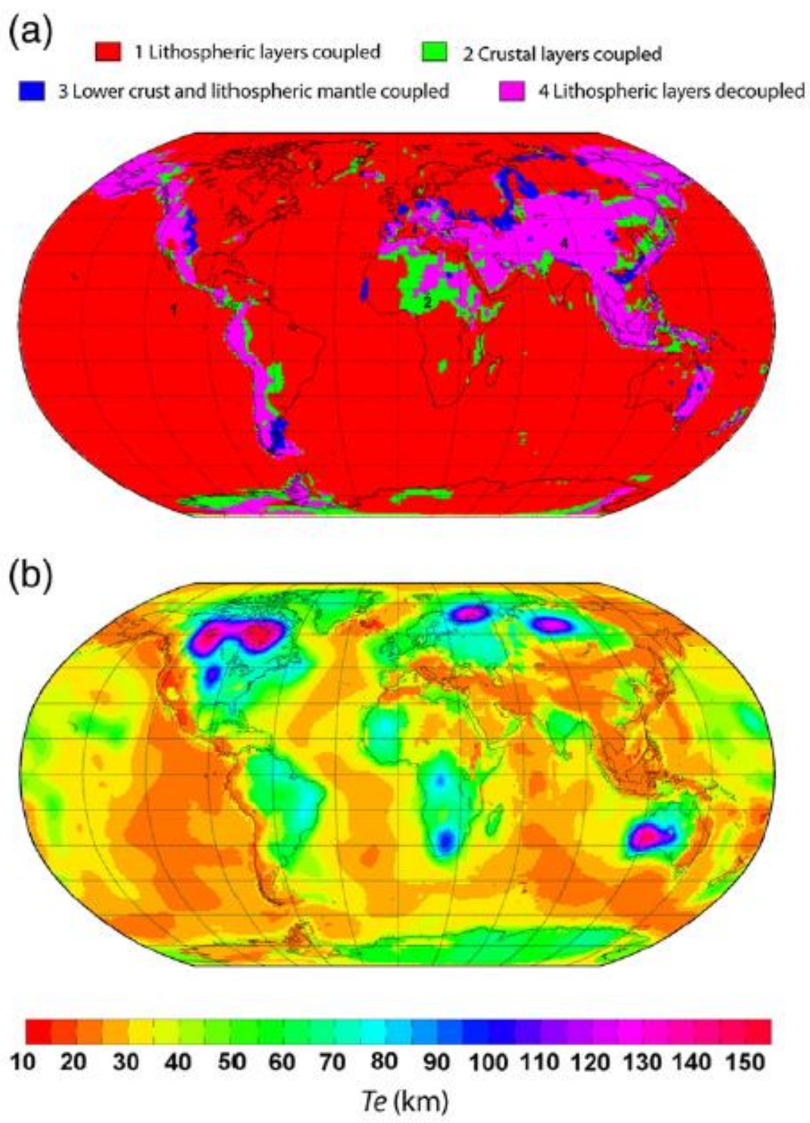

Fig. 4. (a–b) (a) Coupling and decoupling conditions of the lithospheric layers; (b) Effective elastic thickness (*Te*) of the lithosphere (km).

The *Te* distribution in the oceans (Fig. 4b) reflects the variation of lithospheric strength, with the highest values (40 km) observed in the oldest oceans. In contrast, there is no clear *Te*-age relationship for the continental lithosphere. Instead, variations in *Te* of the continental lithosphere reflect its long complex history. The closure and opening of oceanic basins resulting from assembly and breakup of supercontinents strongly affect the continental margins, which are repeatedly weakened by thermal rejuvenation and fault reactivation during subduction, orogeny and rifting. In contrast, continental cores are left mostly undeformed. Therefore, *Te* in the continental areas is primarily related to the combined effects of rheological and thermal heterogeneity, which controls coupling or decoupling conditions of the lithospheric layers (Fig. 4a). The *Te* distribution for the continents (Fig. 4b) is bimodal with peaks at ~25 km, a representative value outside the cratons, and at ~70 km, a common value for the cratons. This clustering results from the vertical distribution of strength: depending on the ductile strength of the lower crust, the upper continental crust is mechanically coupled or decoupled from the mantle, resulting in very different *Te* values. Large changes of *Te* occur across sutures that separate provinces with major differences in strength. For example, crust–mantle decoupling drastically reduces the total integrated strength and *Te* (~40 km or over) of the lithosphere over the short (~100 km) transition from the interior of the North and South American plates to the Cordillera. This reduction implies a possibility of lateral flow in the lower crust enhanced by other processes (e.g. grain-size reduction) (Burov et al., 1993). These results agree with most admittance and coherence (Pérez-Gussinyé, and Watts, 2005; Swain and Kirby, 2006; Tassara et al., 2007; Audet and Burgmann, 2011) studies, which find that *Te* of cratons is significantly larger (>60 km) than their mean crustal thickness (~40 km).

Espessura elástica efetiva

Effective elastic thickness of South America and its implications for intracontinental deformation

M. Pérez-Gussinyé
Institute of Earth Sciences "Jaume Almera," CSIC, Lluis Sole i Sabaris s/n, Barcelona E-08028, Spain (mperez@ija.csic.es)

A. R. Lowry
Department of Geology, Utah State University, 4505 Old Main Hill, Logan, Utah 84322, USA

A. B. Watts
Department of Earth Sciences, University of Oxford, Oxford OX1 3PR, UK

Geochemistry Geophysics Geosystems G[3]
AN ELECTRONIC JOURNAL OF THE EARTH SCIENCES
Published by AGU and the Geochemical Society

Article
Volume 8, Number 5
16 May 2007
Q05009, doi:10.1029/2006GC001511
ISSN: 1525-2027

Espessura elástica efetiva

Mechanical strength is a fundamental property of the continental lithosphere that controls its response to long term forces and, therefore, the temporal evolution and spatial configuration of continents. It can be parameterized through the flexural rigidity $D \equiv E \cdot Te^3/12(1-v^2)$, which is a measure of the resistance of the lithosphere to flexure in response to loading. Young's modulus, E, and Poisson's ratio, v, are material properties commonly treated as constant (10^{11} Pa and 0.25 in this work). With this assumption, D depends entirely on the elastic thickness Te. This parameter can be defined as the thickness of an 'imaginary' elastic plate overlying an inviscid substratum that would bend by the same amount as the 'real' lithosphere under the same applied loads.

Comparing values of Te estimated from thin elastic plate rheology and surface observables (e.g. direct observations of deflection, gravity anomalies, seismic images) against more realistic rheological models (brittle– elastic–ductile) has proved to be a powerful tool for constraining the role played by different factors (e.g. compositional structure, geothermal gradient, tectonic forces) that influence lithospheric dynamics.

Método usado

- the continuous wavelet transform (CWT) for spectral isostatic analysis.
- we first computed a Bouguer anomaly grid from the global gravity model EIGEN-CG03C that combines terrestrial/marine gravity data with results of the CHAMP and GRACE satellite missions. Transforma dados de anomalia ar-livre em anomalia Bouguer, usa um plato e topografia e batimetria de satélite, e densidades de 2670 kg/m^3 continental e 1650 kg/m^3 para oceano.
- We validate the use of these data by observing that the derived Bouguer anomaly compares well with terrestrial gravity data for the Central Andes region, and that both databases give similar estimates of Te.

Dados – basicamente gravimetria

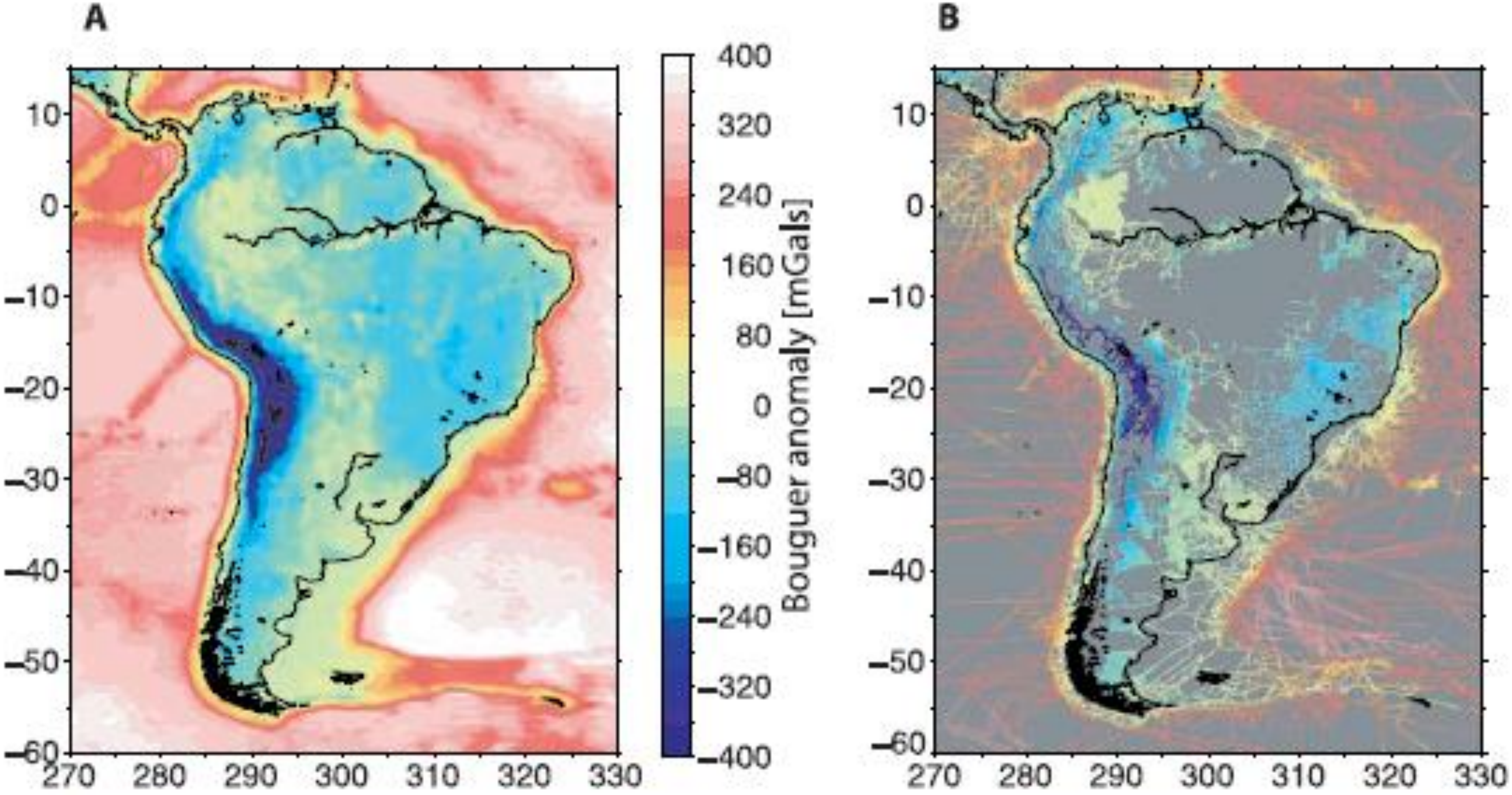

Figure 2. Figure 2a is the final Bouguer anomaly after merging the SAGAP data points shown in Figure 2b with the global model of 1° of resolution: EIGEN-CG30C, obtained from CHAMP and GRACE satellites and terrestrial data [*Foerste et al.*, 2005]. See text for a discussion on the procedure to obtain the Bouguer anomaly.

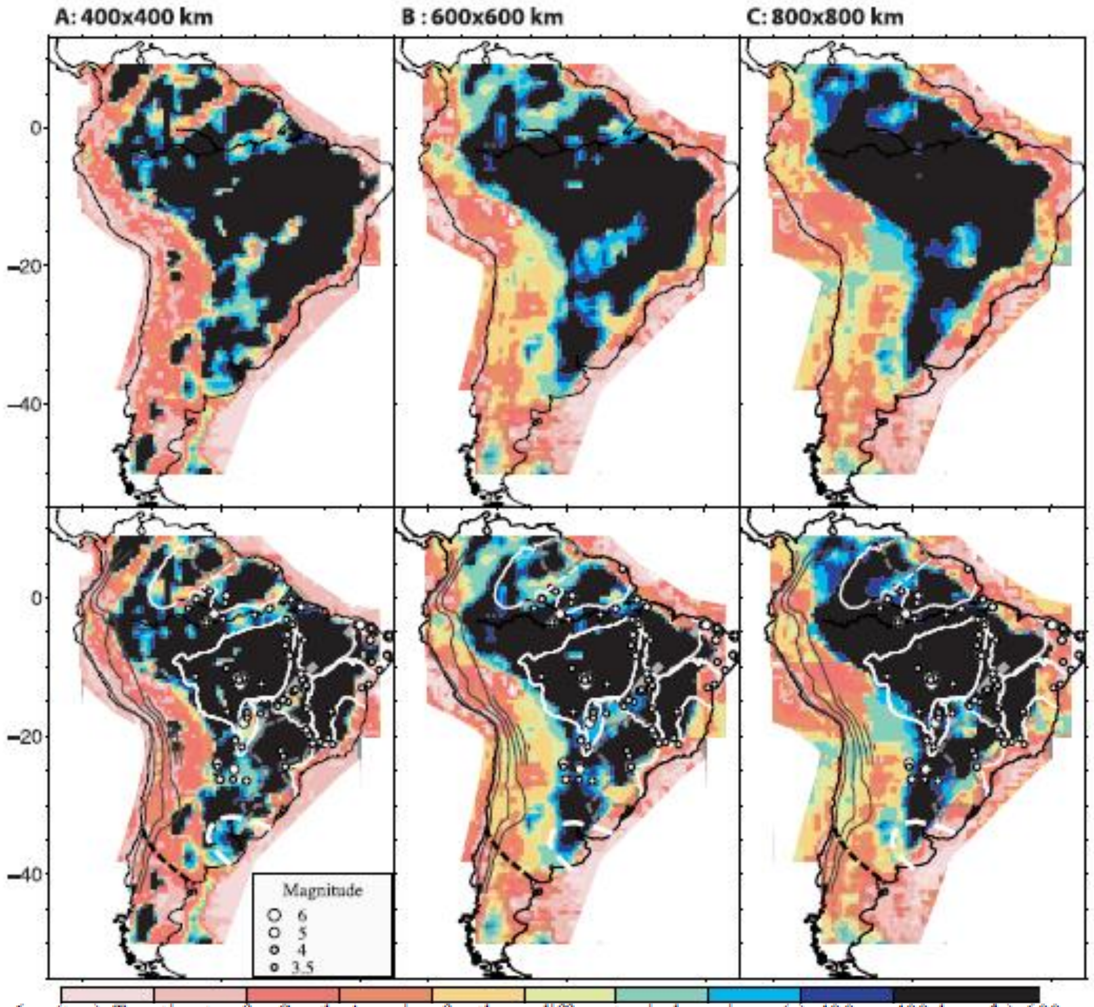

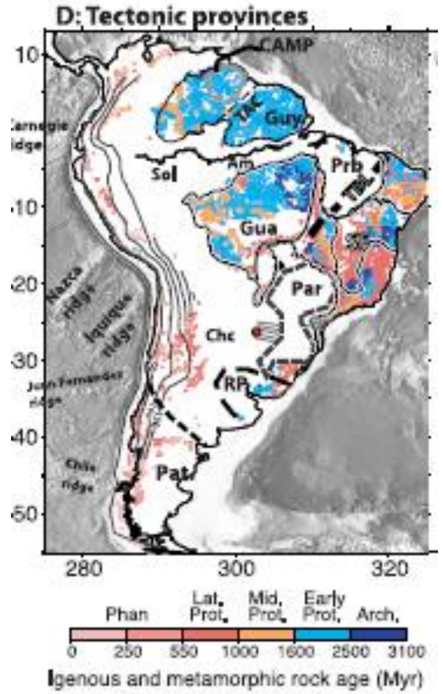

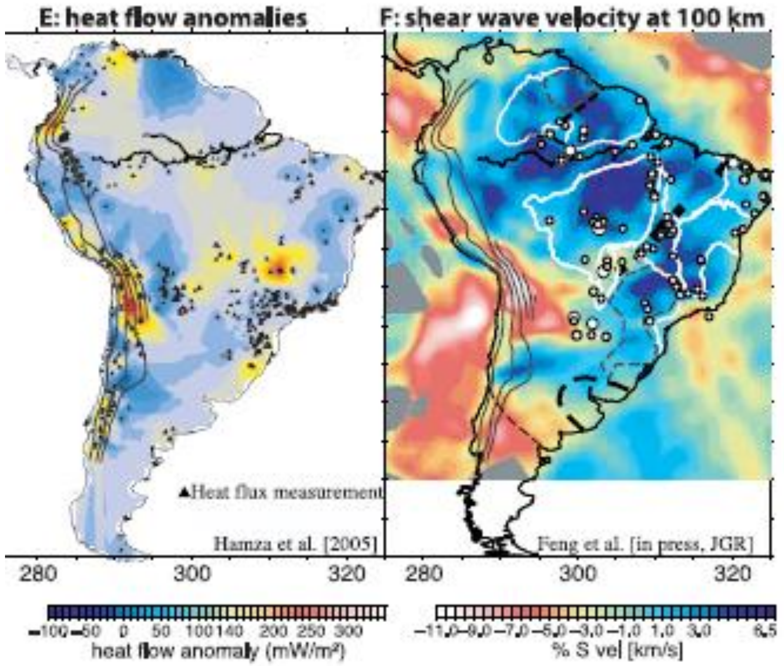

Figure 6. (top) T_e estimates for South America for three different window sizes, (a) 400 × 400 km, (b) 600 × 600 km, and (c) 800 × 800 km, and multitaper parameters of NW = 3 and 5 tapers. (Note that black colors indicate indeterminately large T_e). (bottom) The same as in top, but T_e is superimposed by a normalized catalogue of earthquakes within Brazil, Paraguay, and Uruguay (see *Assumpçao et al.* [2004] for a description of the normalization), by the depths to subducted slab (50 to 250 km from *Syracuse and Abers* [2006]) and by the main tectonic provinces. (d) Bathymetry of South America offshore, and the age of igneous and metamorphic rocks believed to indicate the age of crustal formation [*Schobbenhaus and Bellizia*, 2001]. These are overlain by the main tectonic provinces and the depths to the slab [*Syracuse and Abers*, 2006]. Abbreviations are as in Figure 1, except for Chc, which is Chaco basin. (e) Heat flow anomaly which results from subtracting a regional heat flow field from the observed heat flow values [*Hamza et al.*, 2005]. Triangles are heat flow measurements. The regional heat flow field is a polynomial representation of the South American heat flow and is meant to represent the first-order increase of 60 mW/m^2 in the Stable Platform to 70 mW/m^2 in the Andes [*Hamza et al.*, 2005]. The heat flow anomaly is superimposed by the depths to the slab [*Syracuse and Abers*, 2006]. (f) Shear wave velocity at 100 km depth [from *Feng et al.*, 2007] superimposed by the tectonic provinces, the seismicity from the normalized catalogue, and the depths to the slab [*Syracuse and Abers*, 2006].

Valor de Te usando um modelo de gravimetria EIGEN-CG30C apenas e os dados da figura 2 (slide 9), que são os dados do mapa gravimétrico da Universidade de Leeds e completados com esse modelo EIGEN-CG30C nos vazios.

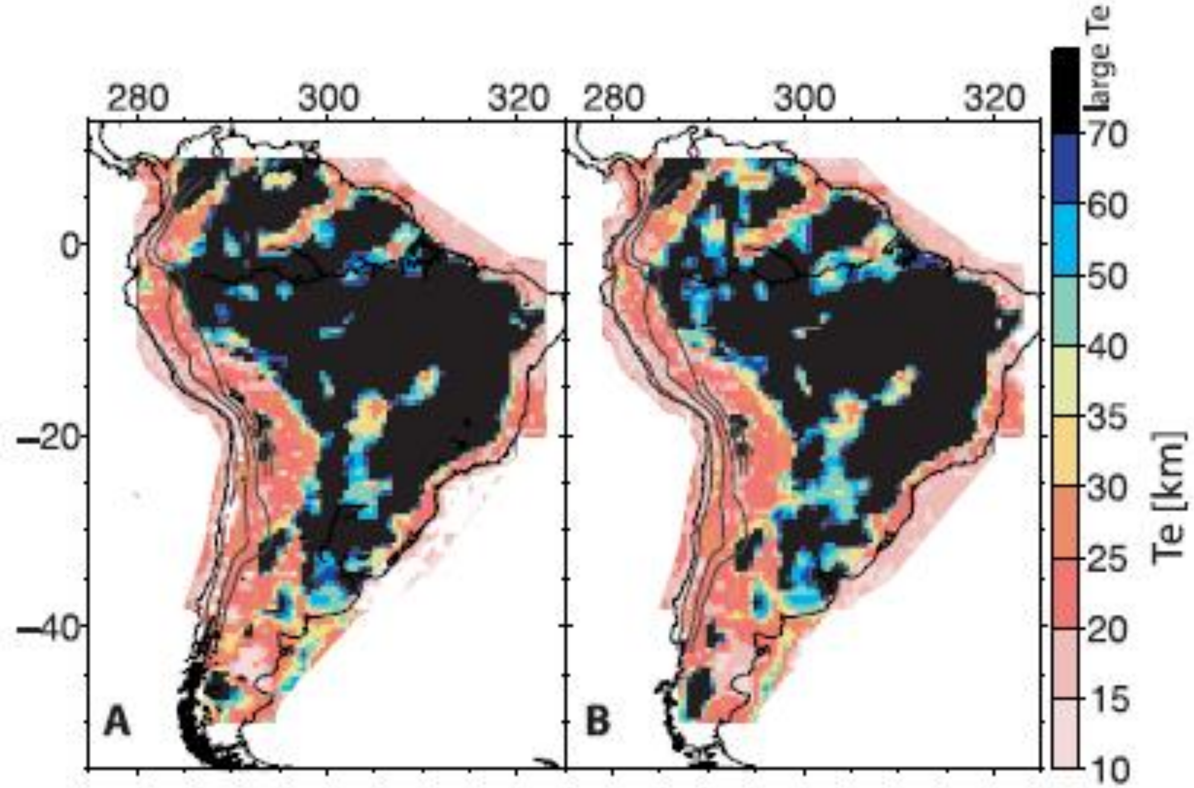

Figure 7. T_e of South America estimated using 400 × 400 km windows and (a) the Bouguer gravity anomaly derived only from the EIGEN-CG30C data. (b) The same as in Figure 7 but using the data generated for this study (see section 3.1). These data result from combining the EIGEN-CG30C-derived Bouguer anomaly and the more detailed SAGAP Bouguer anomaly.

Espessura elástica efetiva

Elastic thickness structure of South America estimated using wavelets and satellite-derived gravity data

Andrés Tassara [a,*], Chris Swain [b], Ron Hackney [c], Jon Kirby [b]

[a] Institut für Geologische Wissenschaften, Freie Universität Berlin, Malteserstrasse, 74-100, D-12249 Berlin, Germany
[b] Western Australian Centre for Geodesy, Curtin University of Technology, GPO, Box U1987, Perth 6845, Australia
[c] Institut für Geowissenshaften, Christian-Albrechts-Universität zu Kiel, Otto-Hahn-Platz 1, D-24118 Kiel, Germany

Available online at www.sciencedirect.com

ScienceDirect

Earth and Planetary Science Letters 253 (2007) 17 – 36

Fig. 1. Geotectonic setting of the study area. Shaded relief image of bathymetry and topography from GEBCO digital data (http://www.ngdc.noaa.gov/mgg/gebco/gebco.html). Thick and thin bold lines are boundaries of large (SA, South America; CA, Caribbean; NA, North America; AF, Africa; SC, Scotia; AN, Antarctica, NZ, Nazca; CO, Cocos) and small (pm, Panama; na, Northern Andes; ap, Altiplano) tectonic plates from model PB2002 (ftp://element.ess.ucla.edu/PB2002) [28]. Arrows depict vectors of plate motion with respect to the hotspot reference frame from model HS3-NUVEL1A [29] as calculated at the given position with the Plate Motion Calculator (http://sps.unavco.org/crustal_motion/dxdt/nnrcalc/). White triangles are active volcanoes (http://www.volcano.si.edu/gvp/world). Diverging grey arrows shows boundaries and names of Andean segments. Dotted lines mark the extent of Achaean to Early Proterozoic cratons. This latter information and the track of the Transbrasiliano Lineament were taken from [30] and [31]. The dashed line oblique to the Southern Andes marks the northern limit of the Patagonian terrain. Over the oceans, thin lines with white numbers mark isochrons of the oceanic lithosphere [32] and names depict major oceanic ridges. Some Andean morphotectonic units are highlighted; Sierras Subandinas (sa), Eastern Cordillera (ec), Santa Barbara System (sb), Sierras Pampeanas, North Patagonian Massif (npm).

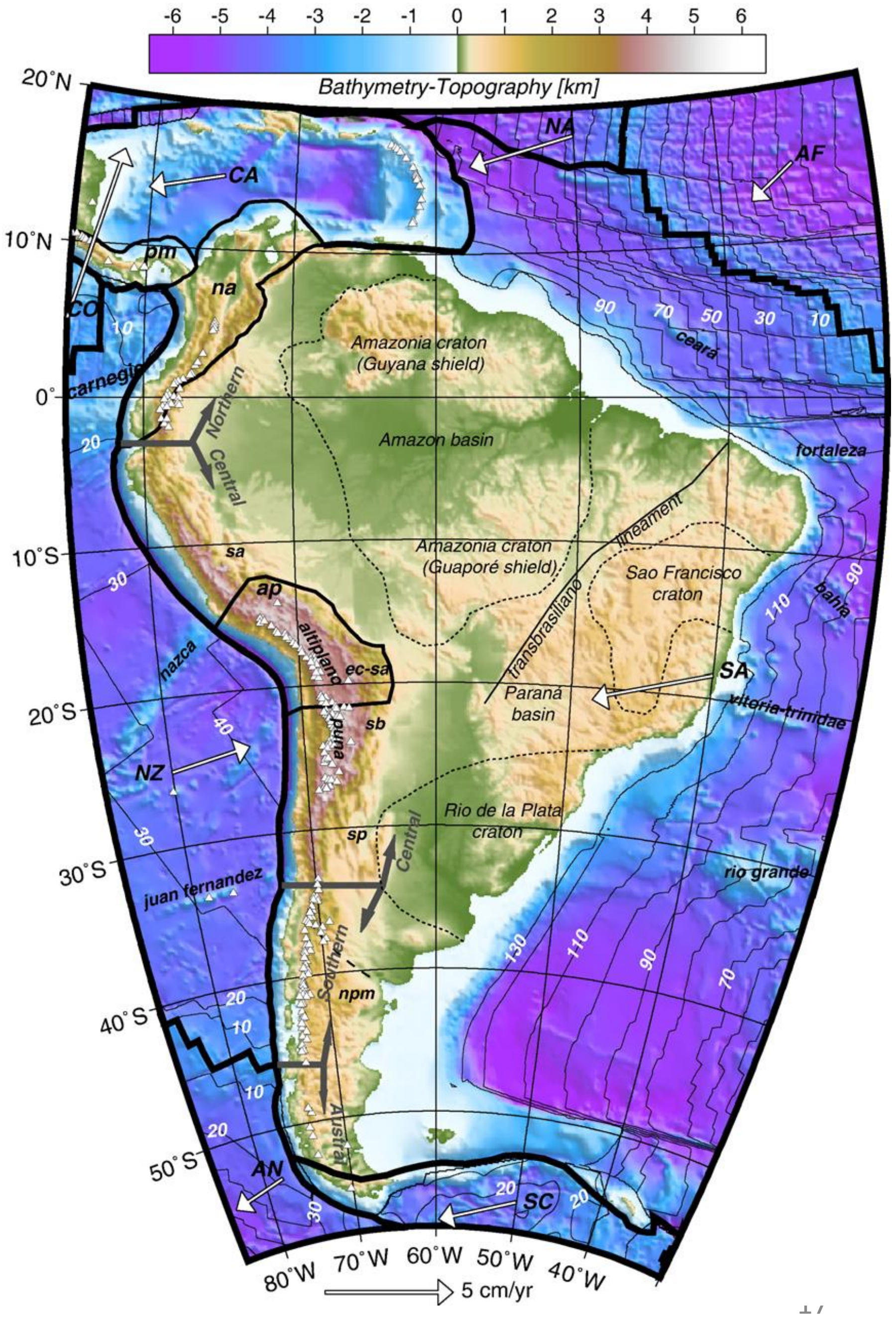

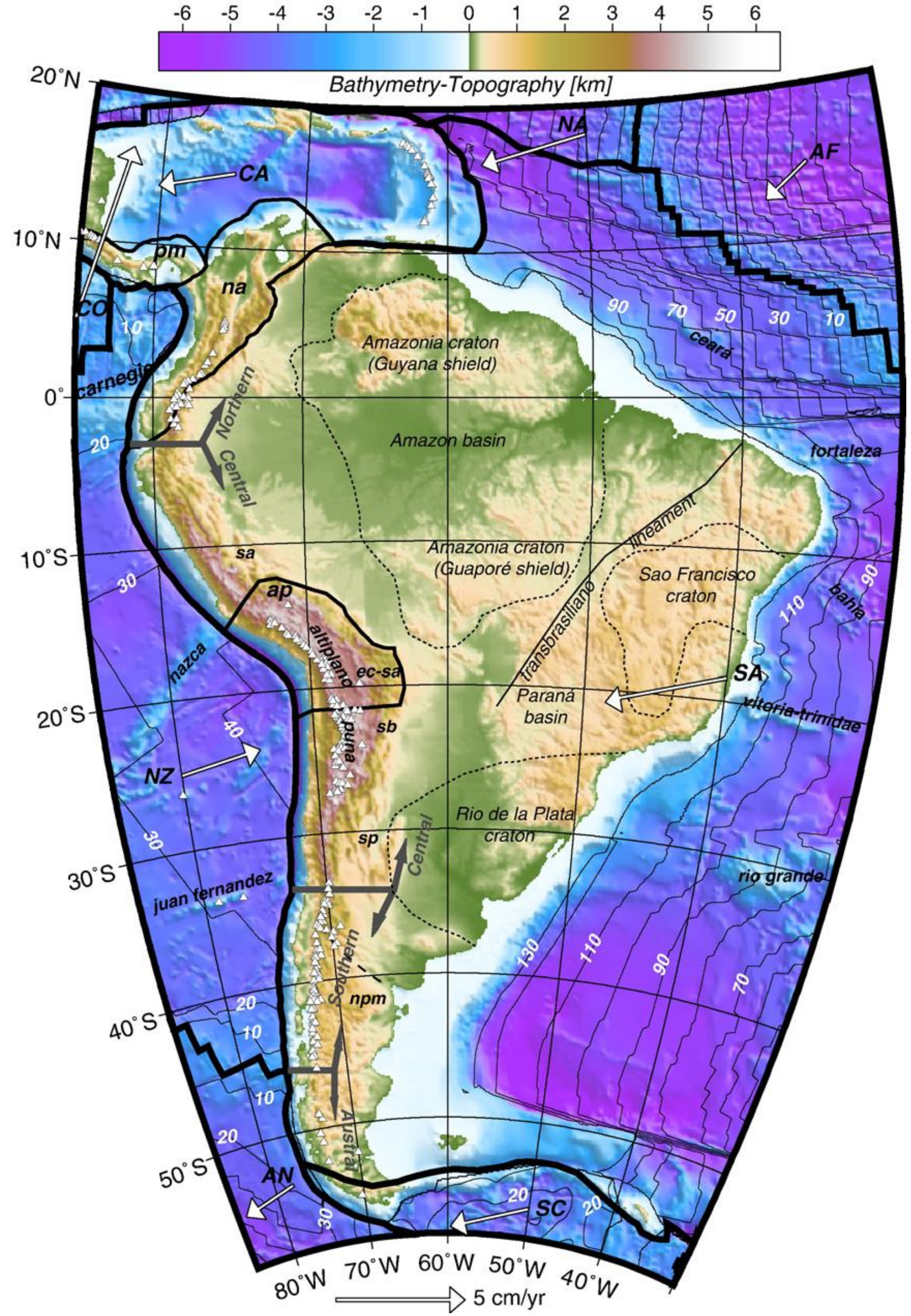

-6 -5 -4 -3 -2 -1 0 1 2 3 4 5 6
Bathymetry-Topography [km]
20°N
10°N
0°
10°S
20°S
30°S
40°S
50°S
80°W
70°W
60°W
50°W
40°W
5 cm/yr
NA
AF
CA
CO
pm
na
carnegie
Amazonia craton
(Guyana shield)
Amazon basin
Northern
Central
ceara
fortaleza
lineament
Amazonia craton
(Guaporé shield)
Sao Francisco
craton
transbrasiliano
bahia
sa
ap
altiplano
ec-sa
nazca
SA
Paraná
basin
vitoria-trinidae
NZ
sb
puna
Rio de la Plata
craton
sp
Central
rio grande
juan fernandez
Southern
npm
Austral
AN
SC

3

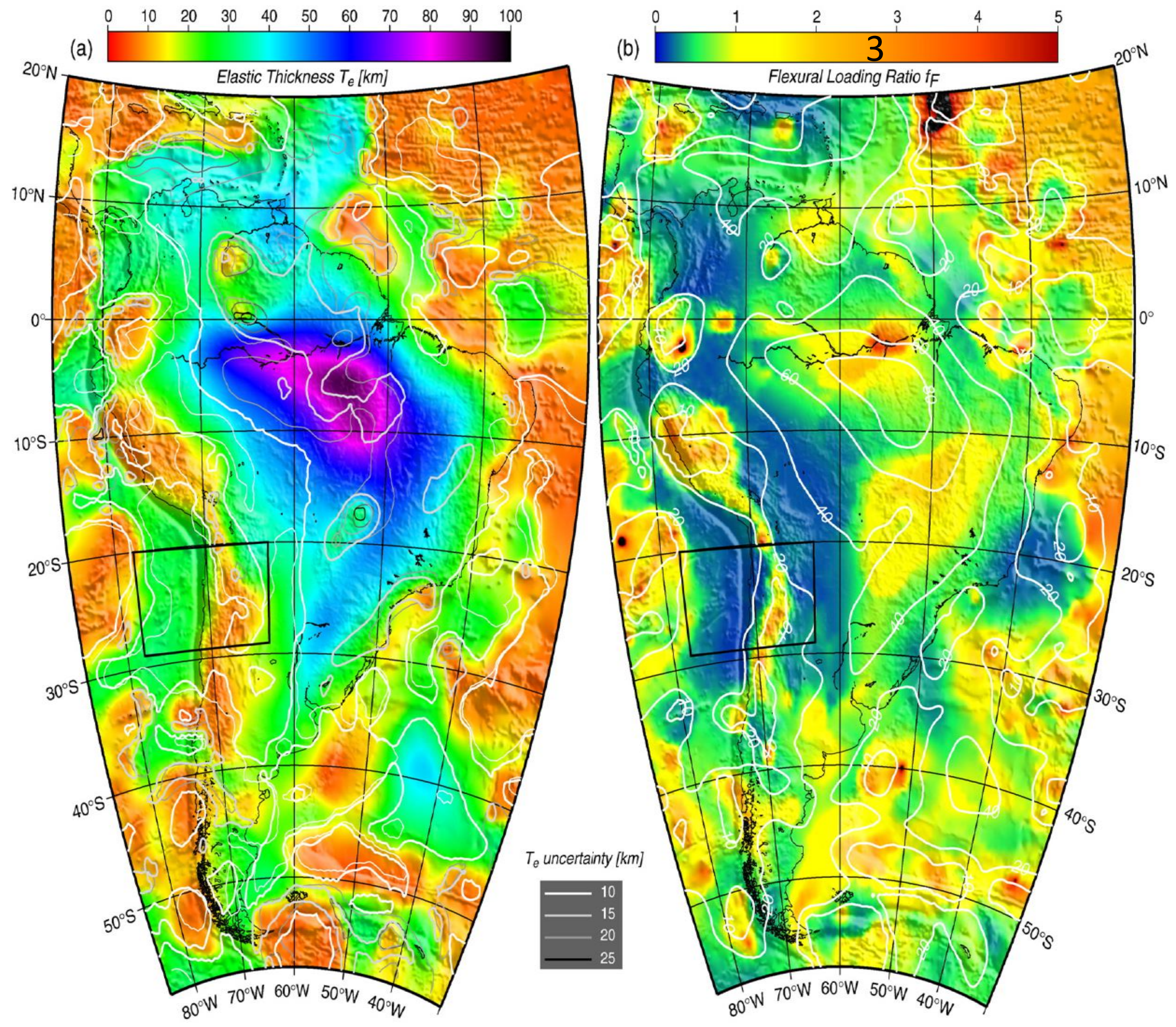

Fig. 3. (a) Computed elastic thickness map (colours) with contours depicting the estimated uncertainty as described in the legend. (b) Com flexural loading ratio f_F (colours) at the transition coherence wavelength (λ_F) contoured with elastic thickness. Both maps are superimpos shaded relief. The box outlines the region shown in Fig. 4.

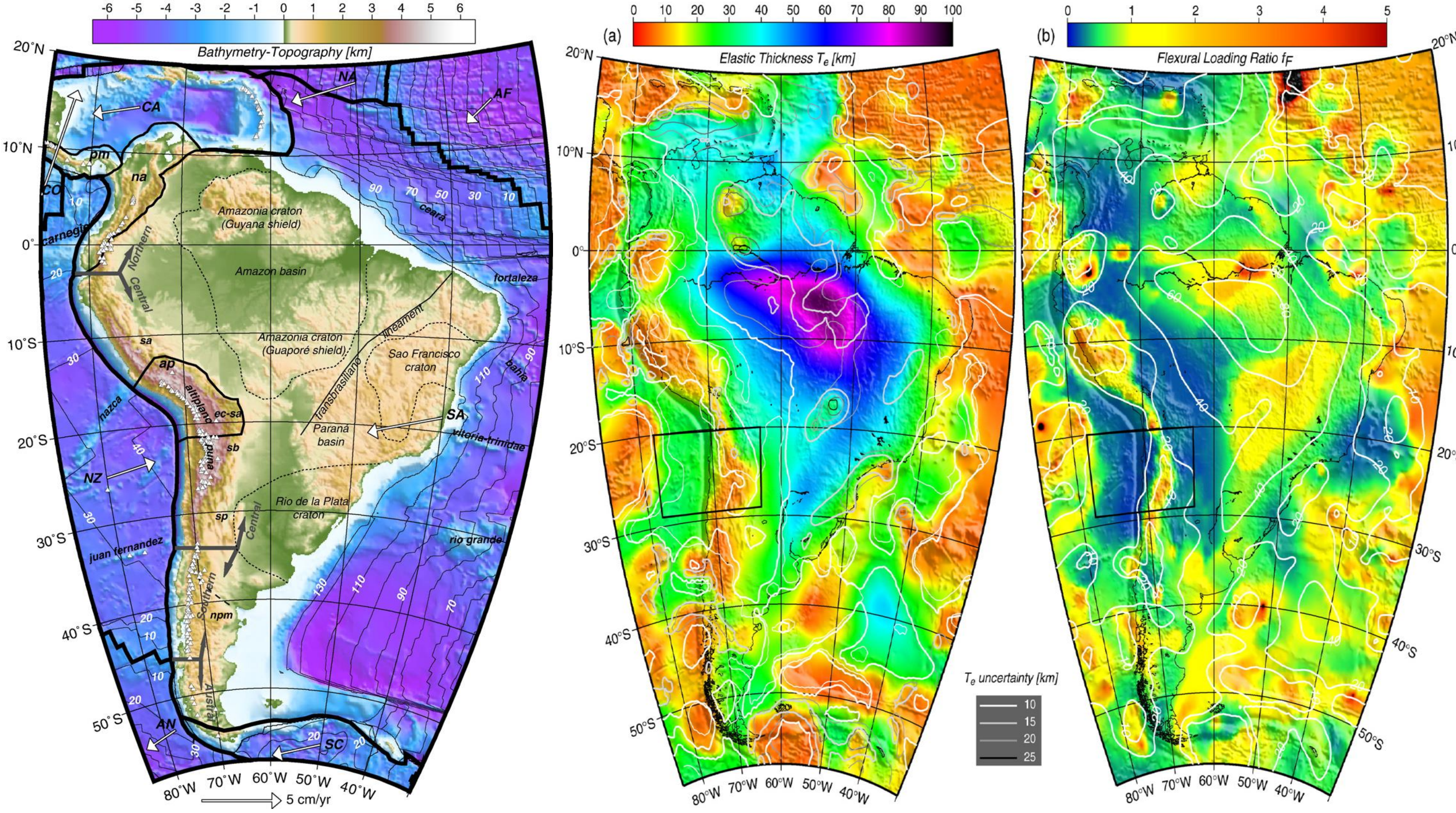
Bathymetry-Topography [km]
-6 -5 -4 -3 -2 -1 0 1 2 3 4 5 6
(a)
Elastic Thickness T_e [km]
0 10 20 30 40 50 60 70 80 90 100
(b)
Flexural Loading Ratio f_F
0 1 2 3 4 5
NA
CA
AF
CO
pm
na
carnegie
Amazonia craton (Guyana shield)
Amazon basin
Northern
Central
ceara
fortaleza
Amazonia craton (Guaporé shield)
lineament
transbrasiliano
Sao Francisco craton
bahia
sa
ap
altiplano
ec-sa
nazca
SA
Parana basin
vitoria-trinidae
sb
puna
NZ
Rio de la Plata craton
sp
Central
rio grande
juan fernandez
Southern
npm
Austral
AN
SC
5 cm/yr
T_e uncertainty [km]
10
15
20
25

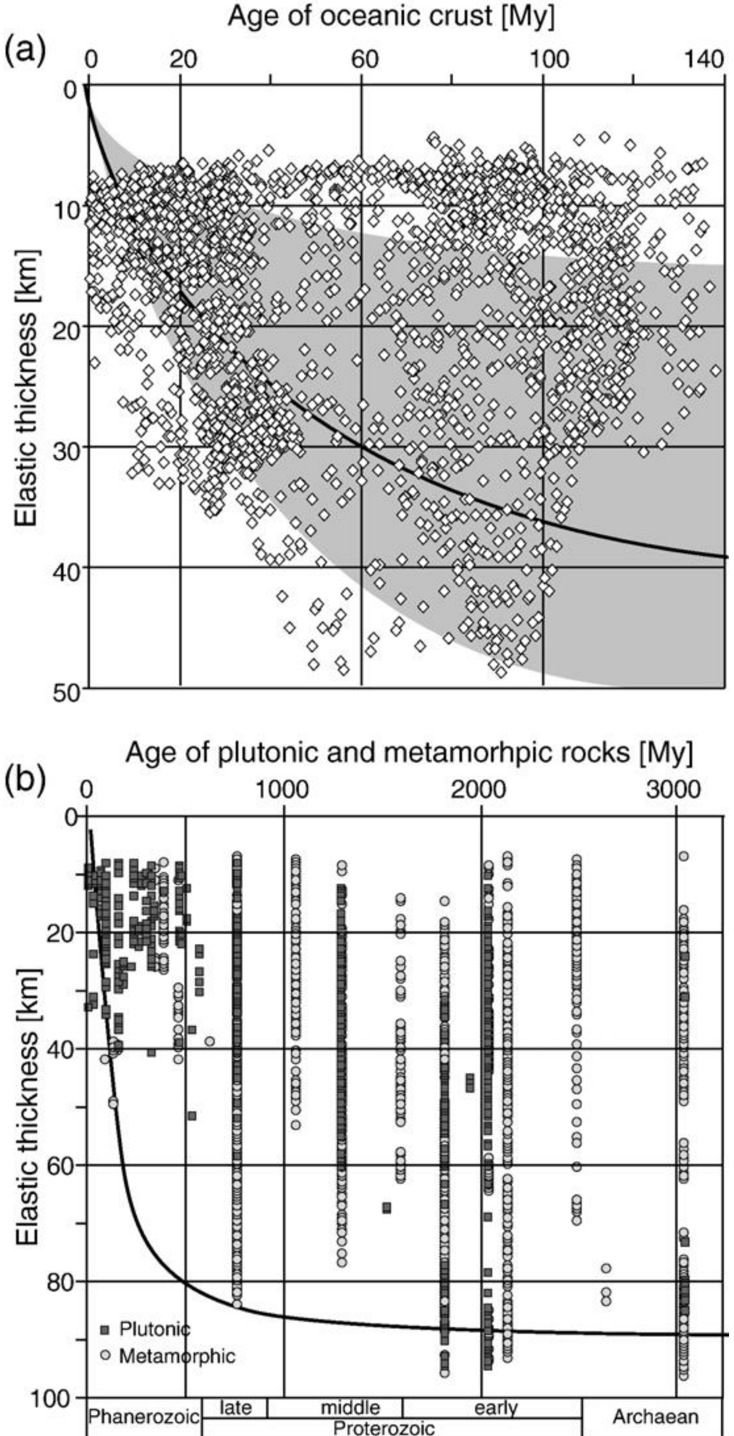

For large areas of the study region, oceanic Te is much lower than the predicted 450 °C isotherm (Fig. 6a).

ΔTe<50% is characteristic of aseismic ridges and should be caused by the thermal rejuvenation of oceanic plates after interacting with deep thermal anomalies like hotspots.

In addition, the loads produced by this interaction (surface volcanism, subsurface intrusions and thermally-induced mantle density changes) were emplaced for some of these ridges early in the thermal evolution of the oceanic plate and our Te estimates should represent the hotter-than-today thermal state of the plate at the time of loading.

Low strength inherited after the continental rifting that separated South America and Africa can similarly explain the low elastic thickness estimated for the oldest oceanic part of the South America plate along the eastern continental margin, where ΔTe can be less than 25%. This has also been observed along other passive margins and explained by the fossilization, as the lithosphere cools, of the loading structure and the low elastic thicknesses characteristically associated with the rifting process.

The oceanic part of the Africa plate analyzed in this study seems to be Significantly weaker (ΔTe<25%) than its South American counterpart. The anomalously low elastic thickness over this region correlates with low seismic velocities at depths of 120–400 km that characterize the region to the east of the Mid Atlantic Ridge north of 0° S. Low seismic velocities at upper mantle depth are primarily caused by high temperatures that, in this case, could be related to the Cape Verde plume.

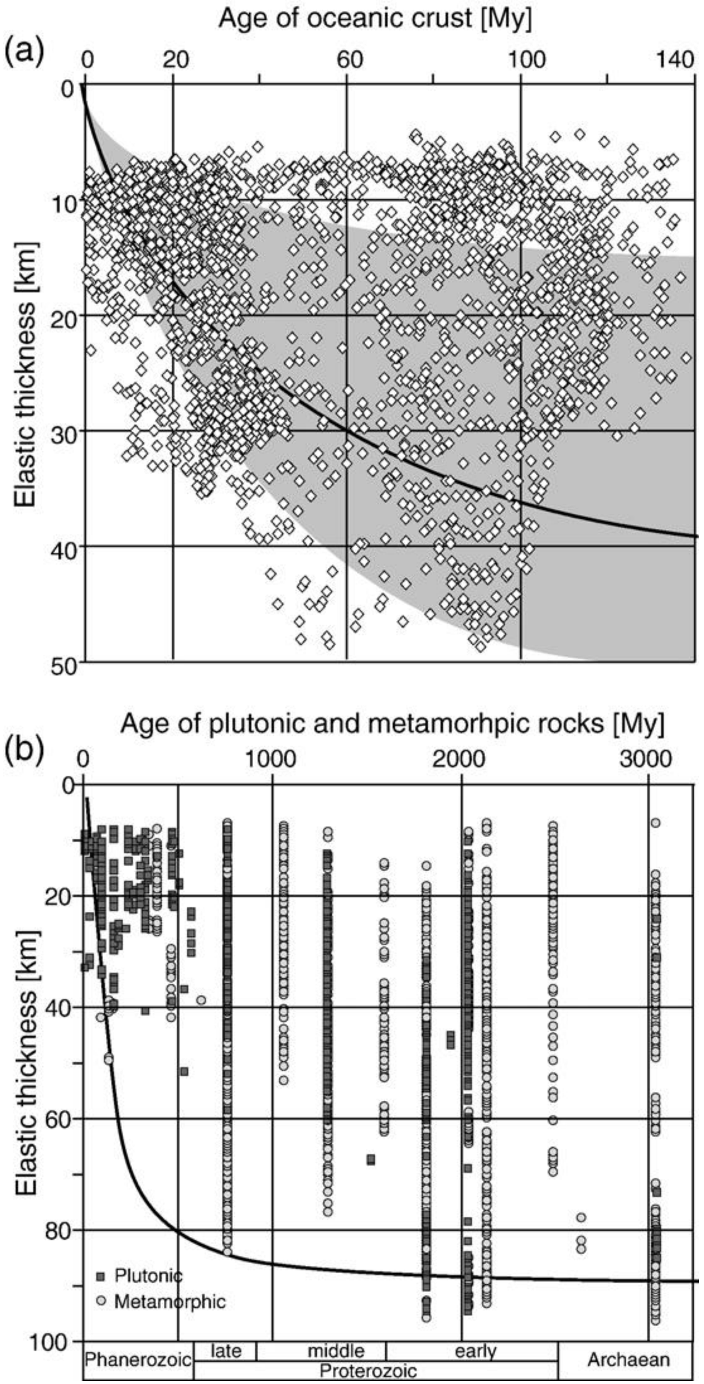

Te estimates of continental areas show a wide range of values defining a weak bimodal distribution with peaks near 20 and 80 km and no obvious correlation with the age of rocks exposed at the surface.

Owing to the continental scale of this database, these averages commonly have a large uncertainty of 30–50%. Fig. 6b also includes the depth to the 450 °C continental isotherm predicted by the age-dependent plate-cooling model with an equilibrium thermal thickness of 250 km. This high thermal thickness is more representative of the continental thermal structure and produces a rapid increase of Z 450°C as the lithosphere becomes older, reaching an asymptotic value near 90 km for ages greater than 1 Gyr. The depth to this isotherm is an upper bound on the elastic thickness and the majority of points analysed in Fig. 6b have Te values much lower than the corresponding Z 450°C. This could be partially due to the uncertainties in the age of crystalline rocks, but we think it is a robust feature demonstrating that the thermomechanical structure of the South American lithosphere has been strongly modified by Phanerozoic tectonic processes.

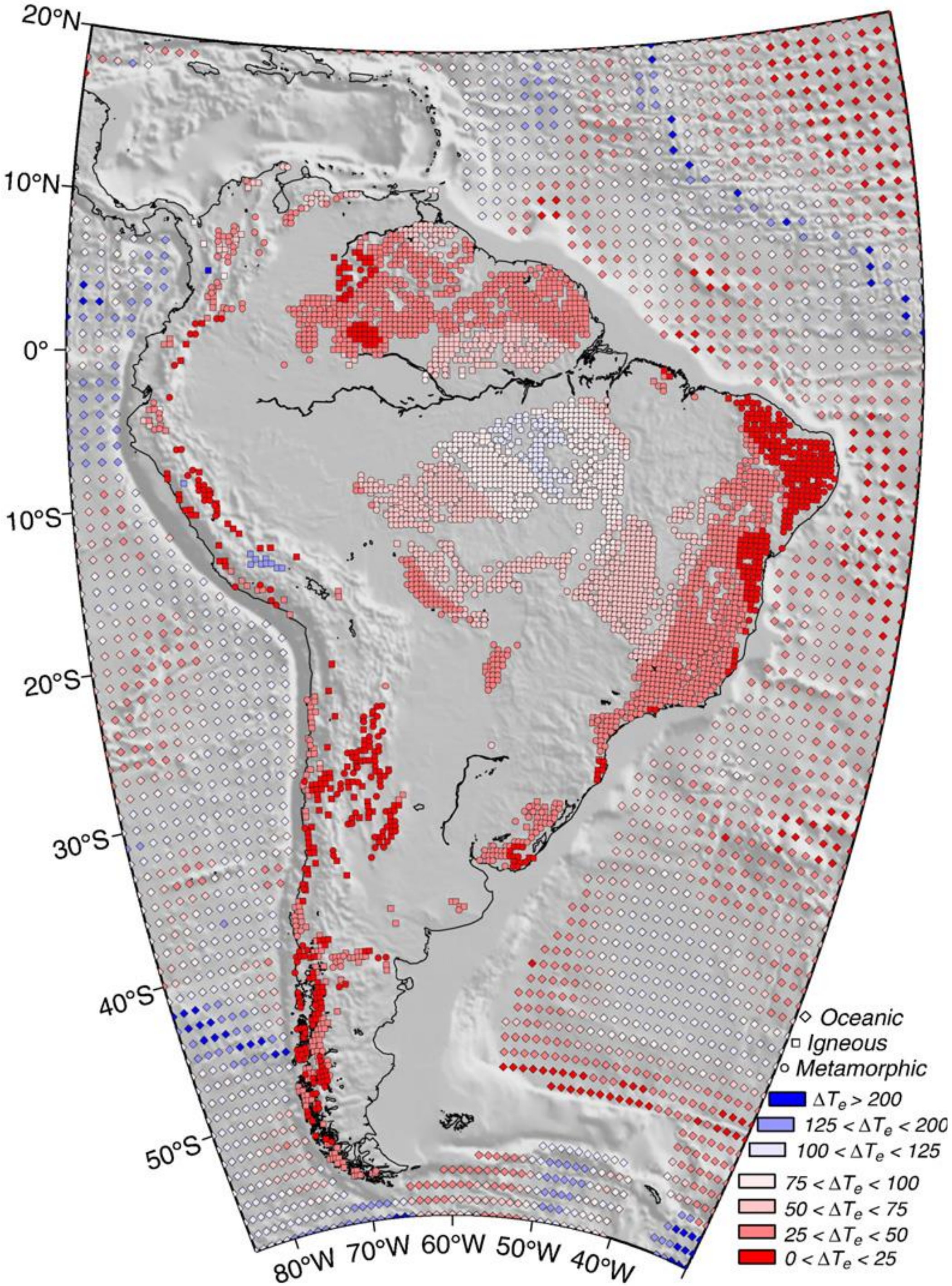

Fig. 7. Map showing the spatial distribution of ΔTe, i.e. the percentage difference between the estimated elastic thickness and the depth to the 450 °C isotherm predicted by a plate-cooling model from the age of oceanic crust (diamonds), and igneous (squares) and metamorphic (circles) rocks on the continent. The equilibrium thermal thickness of the plate-cooling model is 125 km for the oceanic plates and 250 km for the continent. Blue and red colours respectively refer to the case in which Te is higher and lower than the age-predicted depth to the 450 °C isotherm.

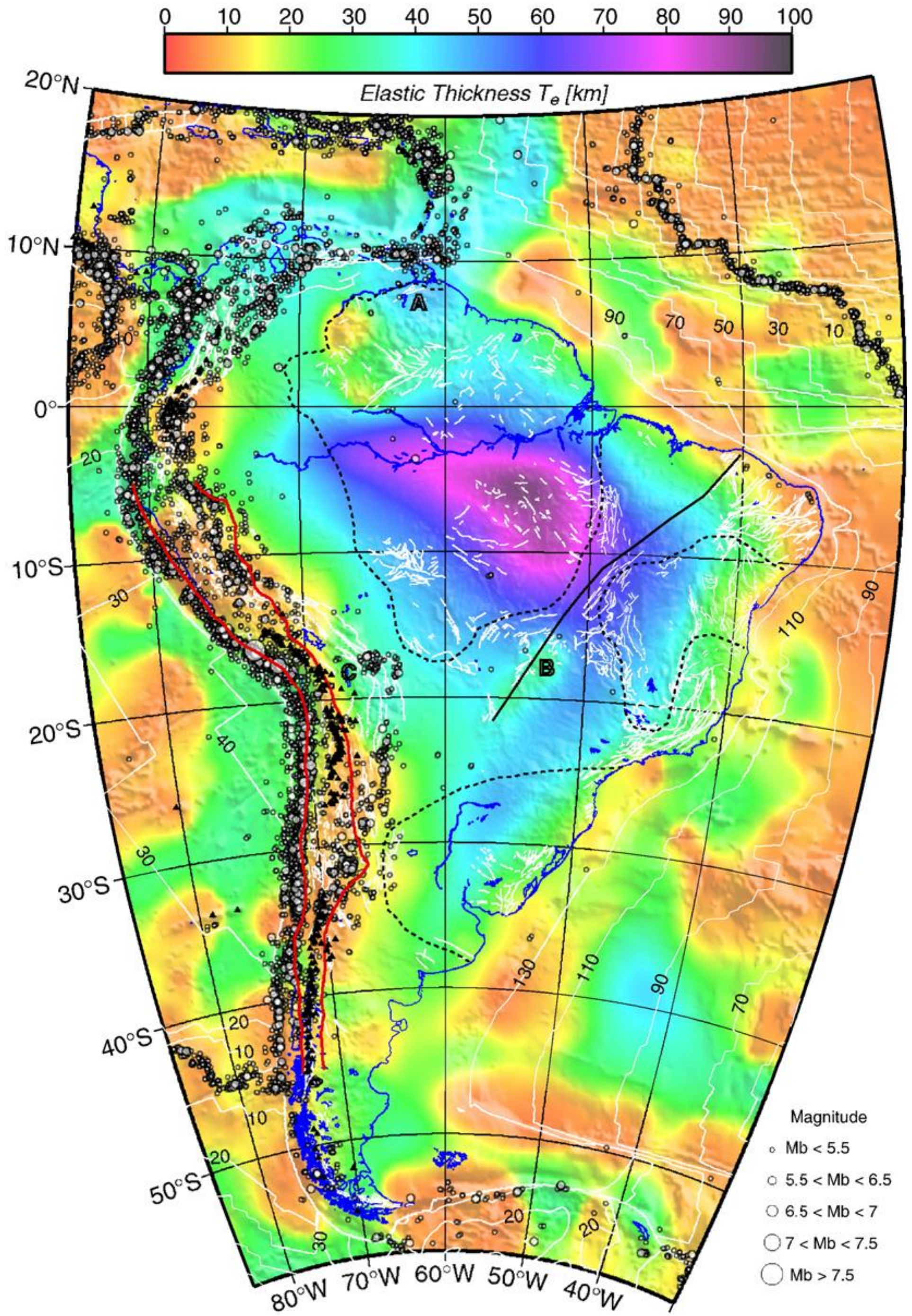

- Finally, our method has, for the first time, mapped the rigidity structure along the continent–ocean transition over a seismically active subduction zone. Comparing this structure with the distribution of earthquakes along the interplate fault, we observe an interesting spatial correlation in which seismic gaps exist where the slab–forearc system seems to be significantly weak (Te<15 km). Owing to the intrinsic incompleteness of the analysed seismicity catalogue, it is difficult at present to propose a physical link between both observations. However, we think that the correlation between the rigidity structure and seismogenic segmentation along the subduction fault suggests a causal relationship that should be investigated in order to improve the understanding and predictability of great earthquakes and tsunamis along the highly-populated Andean margin and other margins worldwide.